The Plant Cell, Vol. 25: 4994–5010, December 2013, www.plantcell.org

Arabidopsis Kelch Repeat F-Box Proteins Regulate Phenylpropanoid Biosynthesis via Controlling the Turnover of Phenylalanine Ammonia-Lyase[C][W][OPEN]

Xuebin Zhang,[1] Mingyue Gou,[1] and Chang-Jun Liu[2]

Biosciences Department, Brookhaven National Laboratory, Upton, New York 11973

Phenylalanine ammonia-lyase (PAL) catalyzes the first rate-limiting step in the phenylpropanoid pathway, which controls carbon flux to a variety of bioactive small-molecule aromatic compounds, and to lignin, the structural component of the cell wall. PAL is regulated at both the transcriptional and translational levels. Our knowledge about the transcriptional regulation of *PAL* is relatively comprehensive, but our knowledge of the molecular basis of the posttranslational regulation of PAL remains limited. Here, we demonstrate that the *Arabidopsis thaliana* Kelch repeat F-box (KFB) proteins KFB01, KFB20, and KFB50 physically interact with four PAL isozymes and mediate their proteolytic turnover via the ubiquitination-26S proteasome pathway. The *KFB* genes are differentially expressed in *Arabidopsis* tissues and respond to developmental and environmental cues. Up- or downregulation of their expression reciprocally affects the stability of the PAL enzymes, consequently altering the levels of phenylpropanoids. These data suggest that the KFB-mediated protein ubiquitination and degradation regulates the proteolysis of PALs, thus posttranslationally regulating phenylpropanoid metabolism. Characterizing the KFB-mediated proteolysis of PAL enzymes may inform future strategies for manipulating the synthesis of bioactive phenolics.

INTRODUCTION

Phenylpropanoids comprise a large family of aromatic metabolites, including the building blocks of the cell wall structural component lignin, and myriad small molecule phenolics, such as coumarins, stilbenes, flavonoids, anthocyanins, and condensed tannins (Vogt, 2010; Fraser and Chapple, 2011), all of which have diverse functions in plant growth and development and plant–environment interactions (Dixon and Paiva, 1995). Many phenolics also have antioxidant activities that can prevent cancer and cardiovascular and neurodegenerative diseases and therefore are beneficial to human health (Winkel-Shirley, 2001; Boudet, 2007; Martin, 2013). The biosynthesis of phenylpropanoids entails a sequence of central enzyme–regulated reactions, from which branch pathways emanate toward different aromatic end products. Multiple levels of regulation control these synthetic processes (Dixon and Paiva, 1995; Martin and Paz-Ares, 1997; Weisshaar and Jenkins, 1998). At the transcriptional level, an array of transcription factors, primarily the MYB, NAC, and WRKY domain–containing proteins, act as positive or negative regulators and constitute a complex, hierarchically organized network, modulating the transcription of the phenylpropanoid-lignin biosynthetic enzymes (Zhong and Ye, 2007; Zhao and Dixon, 2011). In addition, a MYB-basic helix-loop-helix (bHLH) transcription factor-WD40 complex regulates flavonoid-anthocyanin biosynthesis (Broun, 2005). Substantial research has examined the transcriptional regulation of phenylpropanoid biosynthesis, but less is known about the multifaceted regulatory mechanisms controlling phenolic biosynthesis beyond the transcriptional level.

L-Phenylalanine ammonia-lyase (PAL; E.C.4.3.1.5) is the entry point enzyme directing the flow of reduced carbon to the various branches of phenylpropanoid metabolism. It catalyzes the nonoxidative deamination of Phe, yielding *trans*-cinnamic acid (Cochrane et al., 2004). PAL activity determines the flux through the phenylpropanoid pathway and the rate of phenylpropanoid production (Bate et al., 1994). PAL is a tetrameric enzyme; in most species, its subunits are encoded by a small multigene family (Cramer et al., 1989; Wanner et al., 1995). *Arabidopsis* has four PAL members (Wanner et al., 1995; Raes et al., 2003): Three (PAL1, PAL2, and PAL4) exhibit a high binding affinity for Phe and are associated with both the soluble phenolic and tissue-specific lignin synthesis (Rohde et al., 2004; Huang et al., 2010). By contrast, PAL3 has much lower in vitro catalytic efficacy than the other three isozymes and its biological function remains unclear (Cochrane et al., 2004).

In plants, PAL activity is modulated by developmental cues and by biotic and abiotic stresses, such as wounding, UV/blue light irradiation, and infections by fungal pathogens (Dixon and Paiva, 1995). These stimuli affect de novo synthesis of PAL (Edwards et al., 1985) and the inactivation and/or turnover of PAL protein (Tanaka and Uritani, 1977; Bolwell et al., 1985). Earlier studies revealed that environmental factors transiently

[1] These authors contributed equally to this work.
[2] Address correspondence to cliu@bnl.gov.
The author responsible for distribution of materials integral to the findings presented in this article in accordance with the policy described in the Instructions for Authors (www.plantcell.org) is: Chang-Jun Liu (cliu@bnl.gov).
[C] Some figures in this article are displayed in color online but in black and white in the print edition.
[W] Online version contains Web-only data.
[OPEN] Articles can be viewed online without a subscription.
www.plantcell.org/cgi/doi/10.1105/tpc.113.119644

increase the cellular level of PAL; after the initial increase, PAL often rapidly declines to basal or near-basal levels (Tanaka and Uritani, 1977; Lawton et al., 1980; Shields et al., 1982; Jones, 1984), suggesting rapid turnover of the enzyme. In addition, the high concentration of the biosynthetic intermediates of the pathway also causes feedback regulation, triggering the quick decay of PAL activity (Lamb et al., 1979; Shields et al., 1982; Bubna et al., 2011). Those data imply complicated regulation of PAL activity at posttranslational and metabolic levels. However, so far, the molecular nature of the PAL degrading system remains unclear.

The selective degradation of proteins largely occurs via the ubiquitin-proteasome pathway. Ubiquitination-26S proteasome–controlled protein degradation acts as a powerful posttranslational regulatory mechanism, finely tuning diverse eukaryotic cellular processes (Smalle and Vierstra, 2004). Ubiquitin conjugation requires the sequential action of three enzyme complexes: the ubiquitin-activating enzyme (E1), the ubiquitin-conjugating enzyme (E2), and the ubiquitin-protein ligase (E3). Members of the Skp1-Cullin-F-box (SCF) complex class of E3 ligases generally comprise four main subunits: SKP1, Cullin1, RBX1, and one member of the large family of F-box proteins (del Pozo and Estelle, 2000; Lechner et al., 2006). Within this complex, cullin interacts both with SKP1 and RBX1, forming a scaffold on which different F-box proteins assemble. The F-box proteins interact selectively with the target proteins, thereby conferring specificity on the complex (del Pozo and Estelle, 2000). The *Arabidopsis thaliana* genome contains nearly 700 genes encoding predicted F-box proteins (Gagne et al., 2002); these fall into different subfamilies, according to the presence of additional protein–protein interaction domains near the C terminus. One subfamily, the Kelch motif (repeat) containing F-box (KFB) proteins, were initially identified in *Drosophila melanogaster* (Bork and Doolittle, 1994), and more than 270 members have been annotated from *Arabidopsis*, poplar (*Populus trichocarpa*), rice (*Oryza sativa*), maize (*Zea mays*), pine (*Pinus taeda*), and *Physcomitrella patens* (Sun et al., 2007). A few characterized KFBs mainly function in circadian control or in modulating flowering time (Nelson et al., 2000; Han et al., 2004; Somers et al., 2004; Yasuhara et al., 2004; Imaizumi et al., 2005), but their roles in regulating plant secondary metabolism remain unclear.

To gain insights into the molecular basis of the posttranslational regulation of phenylpropanoid biosynthesis and its potential interplay with other biological processes, we systematically explored the potential protein–protein interactions of the phenylpropanoid-lignin biosynthetic enzymes by yeast two-hybrid (Y2H) assays and tandem affinity protein purification–mass spectrometry. Here, we show that three *Arabidopsis* KFB proteins physically interact with and mediate the proteolytic turnover of four PAL isozymes, disturbing *KFB* expression consequently affects the biosynthesis of phenylpropanoids.

RESULTS

PAL Isozymes Physically Interact with KFB Proteins in Vitro and in Vivo

To explore the potential posttranslational regulation of the phenylpropanoid biosynthetic enzymes, we used the Y2H assay to identify their potential interaction partners. For this, we used a set of *Arabidopsis* soluble phenylpropanoid-lignin biosynthetic enzymes as the baits to screen an *Arabidopsis* normalized expression library in yeast cells. With the *Arabidopsis* PAL1 and

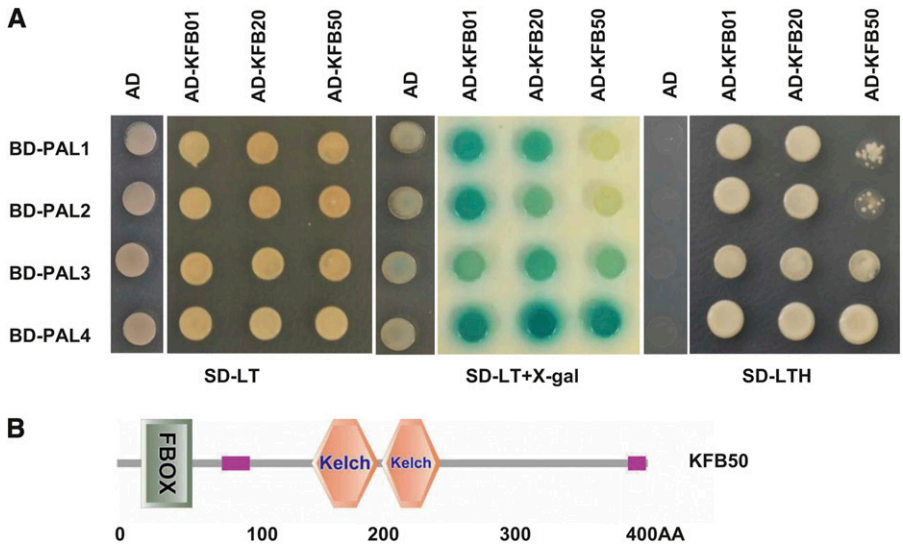

Figure 1. Interaction of PAL Isozymes with Three KFB Proteins in Vitro.

(A) Y2H assay between pDEST-GBKT7-PAL(1/2/3/4) and pDEST-GADT7-KFB(01/20/50). Yeast grown on SD (-Leu/Trp) medium in the presence (middle) or absence of X-gal (left) and on SD (-Leu/Trp/His) medium (right).

(B) Predicted F-box and Kelch repeat domains of the KFB protein.

PAL2 isozymes as baits, we identified interactions with three truncated KFB prey proteins, previously named KFB01, KFB20, and KFB50 (Sun et al., 2007) (see Supplemental Figure 1 online). This observation is consistent with a recent systems biology study exploring the *Arabidopsis* interactome, wherein both KFB01 and KFB50 were found to potentially interact with the PAL enzymes (Arabidopsis Interactome Mapping Consortium, 2011). Each of the three KFB proteins contains a highly conserved F-box motif at the N terminus, which interacts with the SKP1 subunit of the E3 ligase complex (Lechner et al., 2006), and two or three putative Kelch motifs at the C terminus (Figure 1). Subsequently, we amplified the full-length cDNAs of the three KFB proteins and four PAL isoforms and revalidated their pairwise interactions in Y2H assays (Figure 1). The data showed that all four PAL isozymes interact with the three KFB proteins; however, their preferences for interaction appeared slightly different (Figure 1A). In particular, PAL1 and PAL2 preferentially interacted with KFB01 but showed a relatively weak interaction with KFB50, whereas PAL4 displayed a strong interaction with all three KFBs (Figure 1A).

Cytoplasmic Localization of KFB Proteins

PALs are soluble proteins that localize mostly in the cytosol; some isozymes also partially localize on the endoplasmic reticulum surface (Achnine et al., 2004; Bassard et al., 2012). To examine the localization of PAL in our system, we transiently expressed PAL-GFP (for green fluorescent protein) fusions in

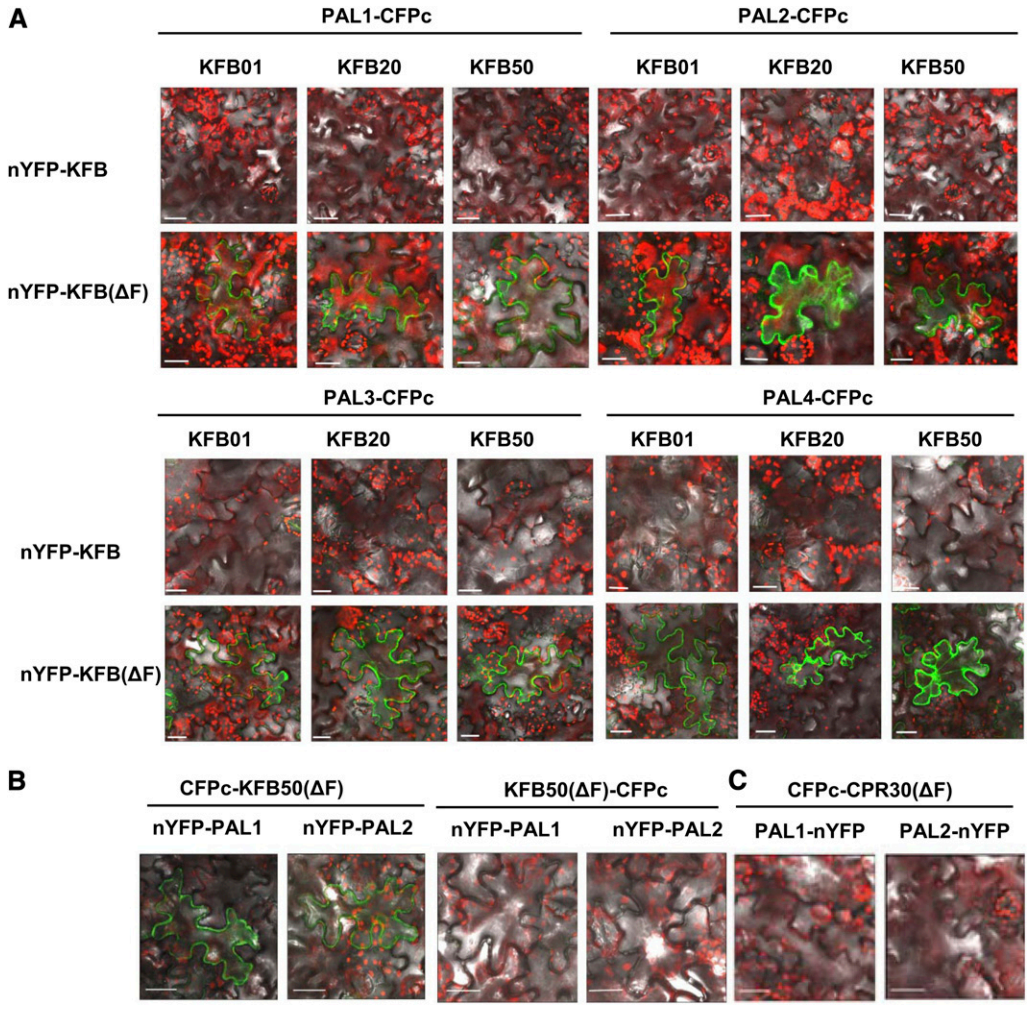

Figure 2. BiFC Assay for the Interactions of PAL Isozymes with KFB Proteins in Planta.

(A) BiFC assay for PAL(1/2/3/4) fused with CFPc at their C termini and KFB (01/20/50) fused with nYFP at their N terminus. The full-length and the truncated KFB(01/20/50) (ΔF) fusion constructs were coinfiltrated with PAL(1/2/3/4)-CFPc constructs in tobacco leaves.

(B) The CFPc tag was fused at either the N or C termini of KFB50. Only CFPc fused to the N terminus of KFB50 gave a BiFC signal when coinfiltrated with nYFP-PAL1/2 constructs.

(C) The truncated F-box protein CPR30 (ΔF) fused with CFPc was used as the negative control.

Bars = 50 μm.

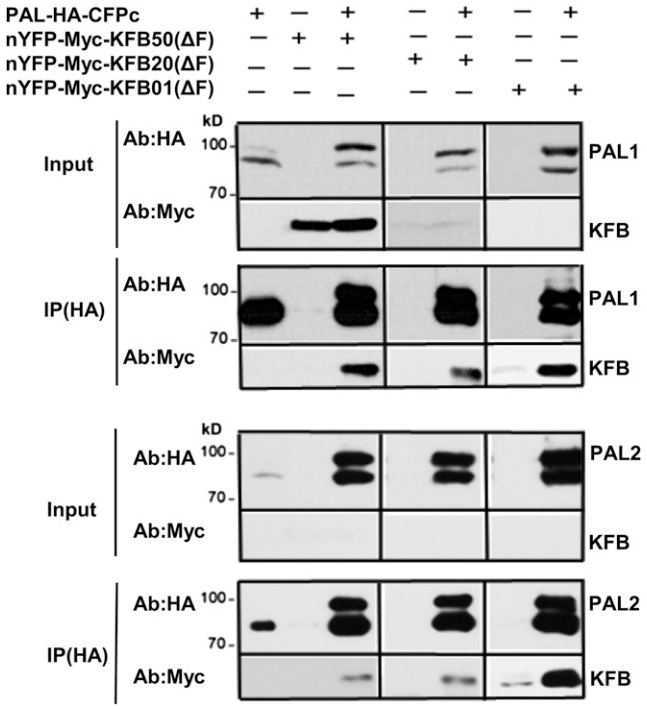

Figure 3. Co-IP of HA-Tagged PAL1/2 with Myc-Tagged KFB01/20/50 Proteins.

Crude lysates (Input) were immunoprecipitated with HA antibody and then detected with HA antibody for PAL tagged with HA and CFPc and Myc antibody for the truncated KFB tagged with Myc and nYFP, respectively. Expected molecular mass of PAL-HA-CFPc fusion is ~100 kD. KFB proteins were present at a low level or were undetectable in the crude lysates but were enriched by immunoprecipitation. Note: In the Co-IP of KFB01, the size of nYFP-Myc-KFB01 overlapped with IgG signal of the HA antibody.

tobacco (*Nicotiana tabacum*) leaves; the PAL-GFP fusions localized primarily to the cytosol and also showed less extensive network-like strand distribution and nuclear periphery localization (see Supplemental Figure 2A online). When the three F-box proteins were fused with GFP either at their N- or C-termini and transiently expressed in tobacco leaves, they also generally displayed a cytosolic distribution, albeit some fluorescence aggregates of AtKFB50-GFP fusion were evident (see Supplemental Figure 2B online). The common cytosolic localization of the full-length KFB and PAL proteins supports their potential interactions in vivo.

PAL Isozymes Interact with KFB Proteins in Vivo

We further examined the interactions of PAL and FKB proteins in planta via bimolecular fluorescence complementation (BiFC), wherein the C termini of the PAL isoforms are fused with the C-terminal half of cyan fluorescent protein (CFPc), while the N termini of either the full-length or the truncated KFB proteins are fused with the N-terminal half of yellow fluorescent protein (nYFP). Surprisingly, coexpression of PAL and the full-length KFB-half fluorescence protein in the leaves of tobacco failed to reveal any complementary chimeric fluorescence signals (Figure 2A). This result indicates that the interaction of a functional KFB with PAL might attenuate the stability of PAL, leading to its rapid turnover. The F-box domain is required to mediate the interaction of the F-box proteins with SKP1 to form a functional SCF-type E3 ligase (Lechner et al., 2006). Subsequently, we created truncated nYFP-KFB fusions, where we removed the predicted F-box domains of KFBs and then coexpressed them with PALs-CFPc. Coexpression of these fusions produced strong chimeric fluorescence signals (at 515 nm) (Figure 2A), pointing to the close proximity or physical interaction of the PAL isoforms with each of the truncated F-box proteins in vivo. When we fused half of CFPc to the C terminus of each of the truncated KFB proteins (rather than to their N terminus) and coexpressed it with nYFP-PALs, there was no BiFC signal (Figure 2B). Although the C-terminal fusion of KFB with a fluorophore fragment might sterically hinder the proper assembly of the two interacting partners, the failure of fluorescence complementation of KFB-CFPc with nYFP-PALs may also indicate that the free C terminus of the KFB proteins is required for recognition of and physical interaction with the PAL proteins. A previous study showed that selective protein interaction requires the C terminus of F-box proteins, which thus specify the ubiquitylation of the targets (del Pozo and Estelle, 2000). In the BiFC assays, we included the F-box protein constitutive expresser of PR30 (CPR30) (Gou et al., 2009) as the control, but we observed no signal when the truncated CFPc-CPR30 fusion protein, whose F-box domain also had been removed, was coexpressed with PAL(s)-nYFP (Figure 2C). This suggests that the BiFC signals in the coexpression of the truncated CFPc-KFB(s) and PAL(s)-nYFP reflect the specific interaction of KFB and PAL.

To further examine whether the PAL and KFB proteins form protein complexes in planta, we conducted coimmunoprecipitation (co-IP) assays with transiently coexpressed PAL and the truncated KFB harboring the hemagglutinin (HA) and cMyc tags, respectively, in tobacco leaf cells. Crude proteins were immunoprecipitated using anti-HA antibody-conjugated agarose beads. Although the three truncated KFBs fused with nYFP-cMyc show low, or even hardly detectable protein levels in the crude cell

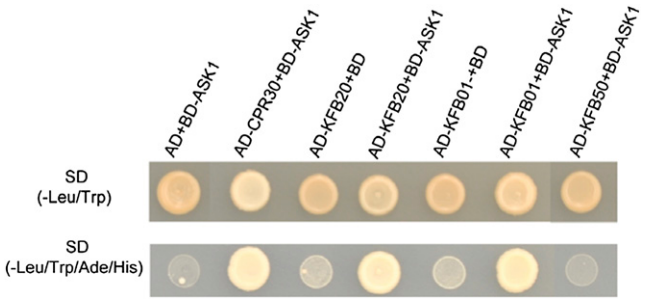

Figure 4. Interaction of *Arabidopsis* KFB Proteins with ASK1 in the Y2H Assay.

Yeast cells were cotransformed with the indicated pair of expression constructs grown on SD (-Leu/Trp) medium **(top)** and SD (-Leu/Trp/His/Ade) medium **(bottom)**. The F-box protein CPR30 was used as the positive control. AD, pGADT7; BD, pGBKT7.
[See online article for color version of this figure.]

lysates (Figure 3, the input), they all were coimmunoprecipitated by the anti-HA antibody when they were coexpressed either with PAL1-HA-CFPc or PAL2-HA-CFPc. Thus, this indicates that the PAL and truncated KFB fusion proteins interact in living cells. To confirm that the co-IP of the half YFP- or CFP-tagged fusion proteins does not reflect the spontaneous assembly of the tagged fluorophore fragments, we included a negative control wherein a truncated CPR30 (Gou et al., 2009), with its F-box domain deleted, was fused to a YFP-cMyc tag, as was the truncated KFB. We coexpressed the control fusion with PAL1-HA-CFPc and found that co-IP with anti-HA antibody produced no signal for nYFP-cMyc–tagged CPR30 detected with the anti-Myc antibody (see Supplemental Figure 3 online). These data confirm the specific interactions of the KFB and PAL proteins in vivo.

Interestingly, when either *Arabidopsis* PAL1- or PAL2-HA-CFPc fusion were transiently expressed in tobacco leaves, we also invariably obtained doublet immunoblot bands, with the upper band having the predicted size of a full-length PAL-HA-CFPc fusion protein (Figure 3; see Supplemental Figure 3 online, the input). Coexpression of PAL-HA-CFPc with the truncated KFB fused with nYFP-cMyc engendered an increase in the amount of doublets detected, particularly the upper band (Figure 3; see Supplemental Figure 3 online, the input). We further examined the identity of the immunoprecipitated doublet proteins by liquid chromatography–mass spectroscopy (LC-MS). We purified the enriched PAL1-HA-CFP fusion protein from the tobacco leaves by SDS-PAGE, excised the major Coomassie blue–staining bands corresponding to the doublet immunosignals, and digested the proteins with trypsin for mass spectroscopy. We detected 443 spectra representing 89 unique peptides with coverage of 55% of the sequence of the PAL1-HA-CFPc fusion protein for the upper band and 373 spectra representing 81 unique peptides with coverage of 52% of the PAL1 fusion for the lower band (see Supplemental Data Set 1 online). Although the incomplete coverage of the LC-MS analysis prevents us from precisely determining the origin of the doublet of PAL fusion protein, one possibility may be the partial degradation of the CFPc tag, since the detectable C-terminal sequence of the lower band appeared shorter than that of the upper band. Coexpression of an inactive nYFP-cMyc-KFB protein might contribute to stabilizing the overaccumulated PAL-HA-CFPc, probably as a result of the reassembly of the half fluorescent proteins with respect to the interaction of PAL and KFB. In addition, we also identified two unique peptides of ubiquitin in both digested samples by LC-MS analysis (see Supplemental Data Set 1 online).

KFB Proteins Interact with SCF Complex Subunit SKP1

In the SCF-type E3 complex, SKP1 bridges between the F-box protein and the scaffold Cullin1, which mediates the ubiquitylation of the target protein (del Pozo and Estelle, 2000). *Arabidopsis* has more than 20 SKP1 homologs. Any given SKP1 protein may interact with many F-box proteins and, conversely, the same F-box protein may bind multiple SKP1 proteins, suggesting the combinatorial potential to form a very large set of SCF complexes (Risseeuw et al., 2003). To evaluate whether the KFB proteins we identified can form SCF complexes, we selected a well-characterized *Arabidopsis* SKP1 homolog, ASK1 (Zhao et al., 2003; Yasuhara et al., 2004) to examine, via the Y2H assay, its potential interactions with the identified KFB proteins. We included the characterized F-box protein CPR30, which interacts with ASK1 (Gou et al., 2009) as the positive control. We found that KFB01 and KFB20, but not KFB50, interact with ASK1 (Figure 4), suggesting that the identified KFB proteins can participate in the SCF complex via their direct interaction with the ASK protein(s) and that KFB50 likely interacts with a distinct set of SKP proteins. The physical interactions of the PAL isozymes with KFB01, 20, and 50 and the capability of those KFB proteins to interact with SKP1, the bridging subunit of the SCF complex, strongly suggest that PALs, the first committed enzyme of the phenylpropanoid pathway, might be controlled by selective degradation via SCF-mediated ubiquitylation and the 26S-proteasome system.

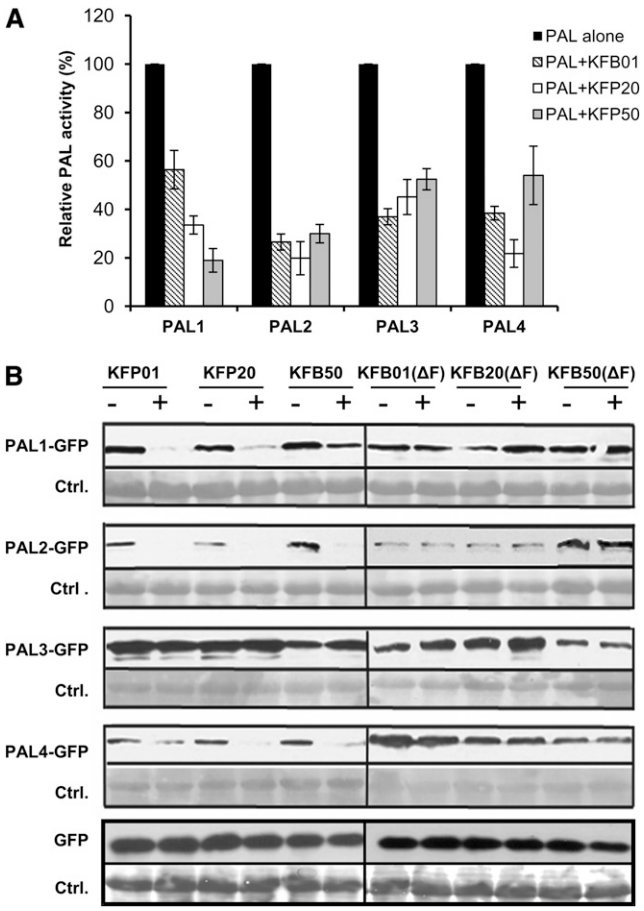

Figure 5. KFB Proteins Attenuate PAL Stability.

(A) The relative activity of expressed PAL isozymes in the crude extracts from the tobacco leaves coexpressing individual *PAL-GFP* and *KFB* genes.

(B) Immunoblot detection of the stability of the PAL-GFP protein using the anti-GFP antibody in tobacco leaves coinfiltrated with *PAL(s)-GFP* and the full-length or truncated *KFB* gene expression constructs. The free *GFP* construct coexpressed with the full-length or truncated *KFB* genes was employed as the control. Ponceau S staining served as the control for the amount of protein loading.

The KFB Proteins Attenuate the Stability of the PAL Isozymes

To evaluate the hypothesis that KFB mediates the turnover of the PAL enzymes, we first examined whether the interaction of the KFB proteins with the PAL isozymes affects PAL activity. We expressed the 35S:PAL(s)-GFP expression cassette both alone and in combination with the 35S:KFB-expressing construct in each half of one tobacco leaf. A GFP expression cassette was included as the control. The multiple half-leaves expressing PAL-GFP or GFP alone with or without KFB were collected and homogenized. The crude protein extracts from the infiltrated leaves were used for measuring PAL enzymatic activity in converting Phe to *t*-cinnamic acid. Coexpression of PAL isozyme-GFP fusion and the individual KFB protein decreased PAL activity by ~50 to ~80% compared with the expression of the individual PAL isozyme (Figure 5A). In agreement with a previous report (Cochrane et al., 2004), the expressed PAL3 exhibited lower catalytic activity than did other isoforms, and the depletion of its measurable activity by the KFB proteins was less severe (Figure 5A).

In verifying whether the reduction of PAL activity resulted from the degradation of PAL protein, we examined PAL-GFP stability by immunoblot with an anti-GFP antibody. The signals for PAL-GFP fusions (~100 kD) were reduced or absent in extracts from leaves coexpressing PAL with individual full-length KFB protein, except for PAL3, which was less affected (Figure 5B). In contrast, we observed no protein degradation when free GFP was coexpressed with each KFB protein (Figure 5B), suggesting the identified KFBs specifically target PAL isozymes. Furthermore, when we coexpressed the PAL-GFP fusion with truncated KFB proteins in which the F-box domains were removed, all the PAL isozymes remained largely intact (Figure 5B). The changes of the PAL activity and stability in the coexpression experiments indicate that three Kelch repeat F-box proteins mediate the selective degradation of the PAL isozymes.

PAL Enzymes Are Degraded via the Ubiquitination-26S Proteasome Pathway

To explore whether PAL degradation occurs via the ubiquitination-26S proteasome pathway, we used a cell-free degradation assay to monitor PAL turnover in the presence and absence of MG132, a specific inhibitor of the 26S proteasome (Yang et al., 2004). Transiently expressed PAL-GFP fusion proteins in tobacco cells (Figure 5) were immunoenriched with the anti-GFP beads and then incubated with crude protein extracts from 6-week-old wild-type *Arabidopsis* stems where active lignification occurs (Ehlting et al., 2005). We used a GFP protein transiently expressed in tobacco leaves as the control. In the absence of MG132, the immunosignals of the PAL-GFP fusion proteins obviously declined or completely disappeared during incubation (Figure 6). Among four PAL isoforms, the in vitro turnover of PAL4 was fastest, and a substantial reduction in its immunosignal appeared within 30 min of incubation with crude protein extract (Figure 6). Applying MG132 substantially blocked or retarded the breakdown of all four PAL isozymes (Figure 6). By contrast, when the enriched free GFP protein was incubated with crude protein extracts from *Arabidopsis* stems in the presence or absence of MG132, its immunosignal remained nearly unchanged throughout incubation (Figure 6). These data demonstrate that the 26S proteasome degrades PAL isozymes.

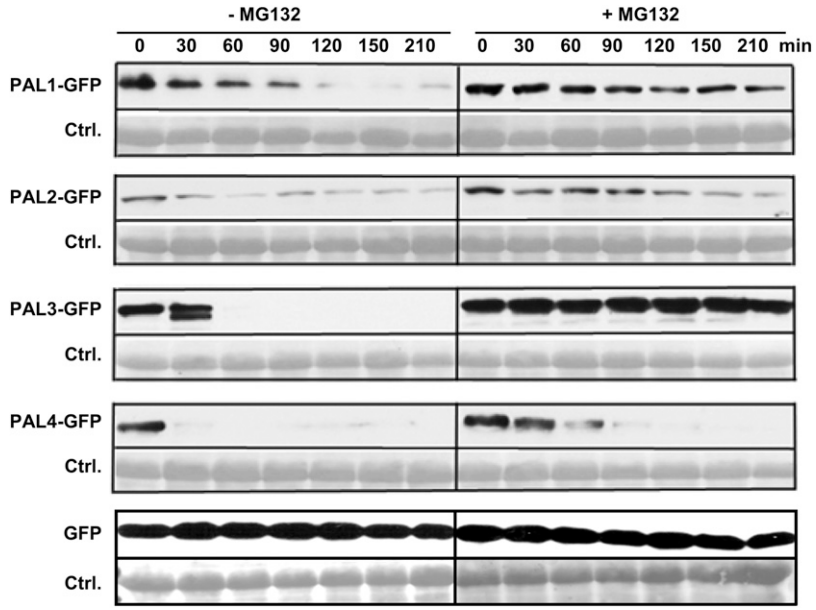

Figure 6. Cell-Free Degradation of PAL Isozymes.

Immunoprecipitation-enriched PAL(s)-GFP proteins from their transiently expressed tobacco leaves were incubated with *Arabidopsis* stem cell lysates in the presence (+) or absence (−) of 0.4 mM MG132. At different times, the level of PAL(s)-GFP was monitored by immunoblot using anti-GFP antibody. The enriched free GFP was taken as the control. Ponceau S staining served as the control for the amount of protein loading.

PAL Isozymes Are Polyubiquitylated in Vivo

F-box protein, as a component of the SCF complex, specifies the targeted proteins for ubiquitylation (del Pozo and Estelle, 2000). The complexity of the SCF type of E3 ligase prevented us from reconstituting the KFB involved ubiquitylation activity specific for PAL isozymes in vitro. Nevertheless, we examined the in vivo ubiquitylation status of these isozymes by transiently expressing the HA-tagged PAL proteins in tobacco leaves in the presence or absence of the MG132 proteasome inhibitor, followed by immunoprecipitation with the HA antibody. When the immunoprecipitated PAL fusion proteins were removed from the anti-HA beads and prepared for loading on SDS-PAGE gel, we found that the conventional harsh treatment (i.e., boiling the bead-bound PAL proteins in SDS buffer) caused nonspecific degradation of PALs and the pull-down of the IgG unit of anti-HA antibody (see Supplemental Figure 4 online). Therefore, we prepared the immunoprecipitated PAL-HA fusion proteins by incubating them with SDS-loading buffer at 42°C; the resulting gel blots respectively were detected by anti-HA- and anti-ubiquitin antibodies. Immunoblotting revealed a few additional anti-HA reactive bands that migrate more slowly than the predicted PAL-HA monomers (~90 kD); by contrast, except for one faint immunoband, probably representing the IgG of HA antibody, no other bands were observed in the mock control, indicating that the bands observed in the immunoprecipitated PAL(s)-HA samples were specific for those carrying the HA epitope (Figure 7A). Correspondingly, when blotted with the antiubiquitin antibody, the immunobands largely overlapped the additional bands detected with the anti-HA antibody and are larger than those of the PAL monomer, pointing to the presence of polyubiquitinated versions of the PAL proteins (Figure 7B). Moreover, MG132 treatment of tobacco leaves enhanced the detectable ubiquitinated PAL-HA proteins in all PAL isozyme extracts (Figure 7). These data suggest that PAL proteins in vivo are ubiquitylated and subject to degradation via the MG132-sensitive 26S proteasome.

KFB Genes Are Differentially Expressed in *Arabidopsis* Tissues

To understand the physiological functions of the three KFBs in planta, we examined their gene expression patterns. Quantitative RT-PCR (qRT-PCR) analysis detected the transcripts of

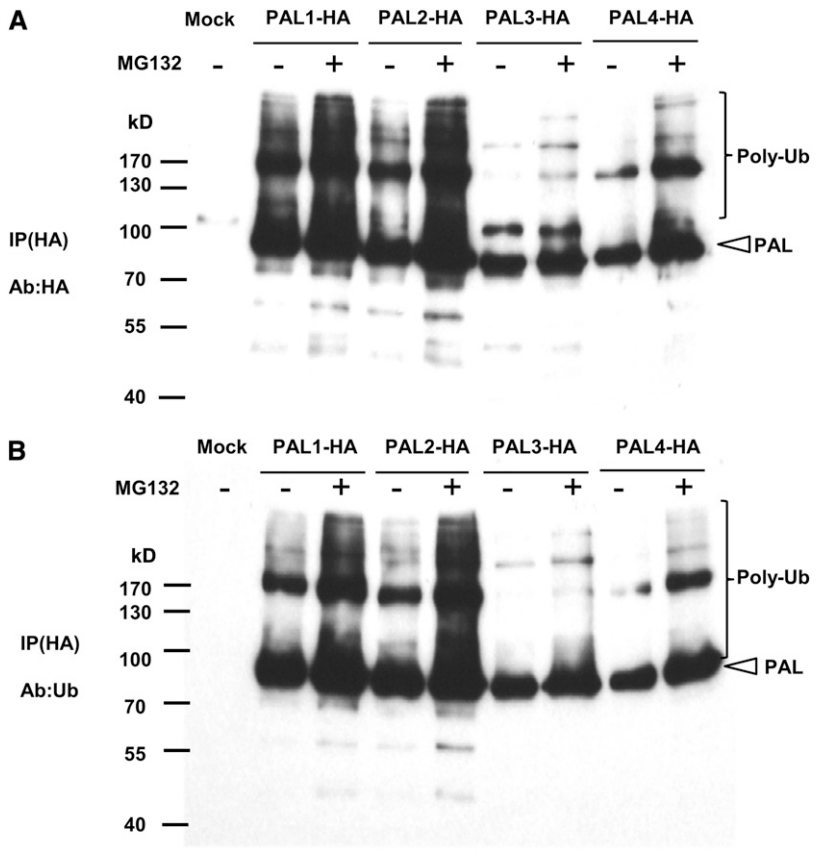

Figure 7. Ubiquitylation of PAL Proteins in Vivo.

Transiently expressed PAL(s)-HA proteins were immunoprecipitation enriched from tobacco leaves preinfiltrated with buffer (−) or with buffer containing 40μM MG132 (+) and then eluted from the IP beads at 42°C. The gel blots were detected by both anti-HA **(A)** and antiubiquitin **(B)** antibodies. A sample that was immunoprecipitation enriched from the buffer-infiltrated tobacco leaf was loaded as the mock control. The PAL-HA proteins and their (poly) ubiquitylated species are indicated. The expected molecular mass for PAL-HA proteins is ~90 kD.

KFB01, *KFB20*, and *KFB50* in *Arabidopsis* stems, rosette and cauline leaves, flowers and buds, and/or siliques but at different levels. As depicted in Figure 8A, *KFB20* strongly expressed in rosette leaves and stems but was low or nearly undetectable in the flower and siliques. *KFB50* was constitutively expressed in all the examined tissues with relatively lower expression in flowers. *KFB01* exhibited overall low expression abundance, but among all the tissues examined, it showed the highest expression in flowers (Figure 8A). The transcripts of *PAL1*, *PAL2*, and *PAL4* universally occurred in leaf, stem, and flower tissues with their predominant expression in the stem (Figure 8A); in addition, the expression of *PAL1* in the flower was also high (Figure 8A). Consistent with a previous study (Rohde et al., 2004), the expression level of *PAL3* was low and its transcript was hardly detected in most of the tissues we examined. In general, the coincidence of the expression of *PAL* isogenes and *KFB* genes in the stem and flower suggests a potential functional relationship between them. Furthermore, we examined the expression of the *KFBs* along with the development of the *Arabidopsis* stem and found that *KFB20* showed highest expression in the developing inflorescence stem where its transcript level was nearly ninefold higher than in the fully developed basal nodes (Figure 8B), implying that developmental cues regulate its expression. *KFB* genes also are expressed in response to environmental stimuli. When *Arabidopsis* seedlings were grown on media containing high carbon (4% Suc), the expression levels of all three *KFB* genes were reduced approximately threefold to ~10-fold compared with those in the seedlings growing on media containing only 1% Suc (Figure 8C). Under such growth conditions, the *PAL* transcript exhibited a moderate induction

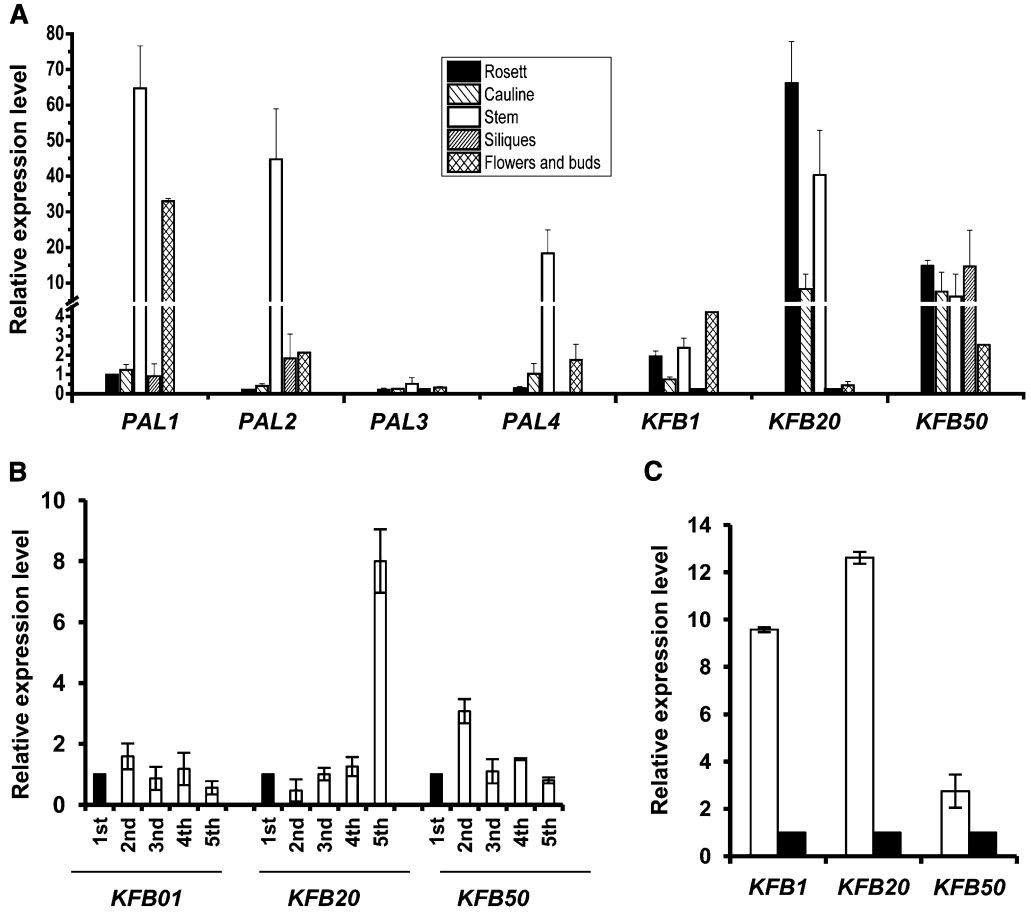

Figure 8. Expression Pattern of *KFB01*, *KFB20*, and *KFB50* in *Arabidopsis*.

(A) The relative expression levels of *KFB01*, *KFB20*, and *KFB50* and *PAL1-4* in different tissues of *Arabidopsis*.

(B) The relative expression levels of the *KFB01*, *KFB20*, and *KFB50* genes in different nodes of the stem. The 1st represents the first basal node above ground of ~6-week-old *Arabidopsis* plants.

(C) The relative expression levels of the *KFB01*, *KFB20*, and *KFB50* in seedlings 5 d after germination growing on one-half-strength Murashige and Skoog medium containing 1 or 4% Suc. The expression level for each gene, after normalization to that of Ubiquitin10 control gene, is expressed as the relative value to the level of *PAL1* in rosette leaves that was expressed as a value of 1 in **(A)** to facilitate the comparison of different genes' transcription, to its level in the first node **(B)**, or to its level in the seedlings grown on high sugar containing medium **(C)**. Data are the means of the three replicates with standard deviations.

(on medium containing 4% Suc), whereas PAL protein level, examined by immunoblotting, showed a substantial increase (see Supplemental Figures 5A and 5B online); consequently, the seedlings growing on the higher carbon source accumulated more anthocyanin pigments (see Supplemental Figure 5C online).

Disrupting the *KFB* Gene Enhances Biosynthesis of Phenylpropanoids

To further explore the biological functions of these *KFB* genes, we examined the T-DNA insertion mutant lines of *KFB01*, *KFB20*, and *KFB50*. RT-PCR analysis indicated that its insertion in the selected mutant lines caused null mutation of the individual *KFB* genes (see Supplemental Figure 6 online). However, those *kfb* single null mutant lines yielded neither a discernible morphological phenotype nor significantly disturbed total PAL activity or deposition of lignin compared with wild-type plants (Figure 9). Speculating about the functional redundancy of those identified KFB proteins in vivo, we created the double and triple mutant lines. Immunoblot analysis against a developed anti-PAL peptide antibody revealed stronger immunoblot signals in the high-order triple mutant lines compared with that in the wild type and single *kfb* knockout mutant lines (Figure 9A), implying that the simultaneous disruption of two or three *KFB* genes increases the cellular level of total PAL proteins and that KFB proteins indeed have functional redundancy in controlling PAL degradation. Correspondingly, the total PAL activities in the multiple mutant lines had risen (Figure 9B). These data suggest that *KFB* expression directly relates to the turnover of PAL proteins in vivo. Examining the content of soluble phenolics and lignin in the double and triple mutant lines, we found a considerable increase in the sinapoyl esters and anthocyanins in young seedlings (Table 1); we also detected a discernible rise in the content of acetyl-bromide lignin in the cell walls of mature triple mutant plants (Figure 9C). Interestingly, the flavonol content in mutant seedlings did not alter significantly compared with its level in wild-type plants, implying that additional regulatory controls might exist on the branch pathways of flavonol synthesis (Table 1).

Overexpression of *KFB* Impairs the Biosynthesis of Phenylpropanoids

To better assess the function of the KFBs in regulating phenylpropanoid biosynthesis, we constitutively expressed individual *KFB* genes, driven by the 35S promoter, in *Arabidopsis* (Columbia-0). We screened the T1 generation of transgenic lines harboring individual *KFB* genes for potential changes of PAL activity in the inflorescence and for the lignin content in the cell walls of their mature stems (see Supplemental Figure 7 online). Despite variation between independent transgenic lines, the total PAL activity in most T1 *KFB*-expressing plants was reduced from 5 to 80% of that of control plants harboring an empty vector (see Supplemental Figure 5 online). In general agreement, the content of acetyl-bromide lignin in the mature stem declined 2 to ~70% in the transgenic lines, as was evident particularly in the *KFB20* overexpression lines (see Supplemental Figure 7 online). In addition, in some of the transgenic lines, the anthocyanin pigmentation seen at the conjunction of the root and rosette leaves and the leaf petioles of the control plants had essentially disappeared (see Supplemental Figure 8 online). These morphological and chemical phenotypes indicate that

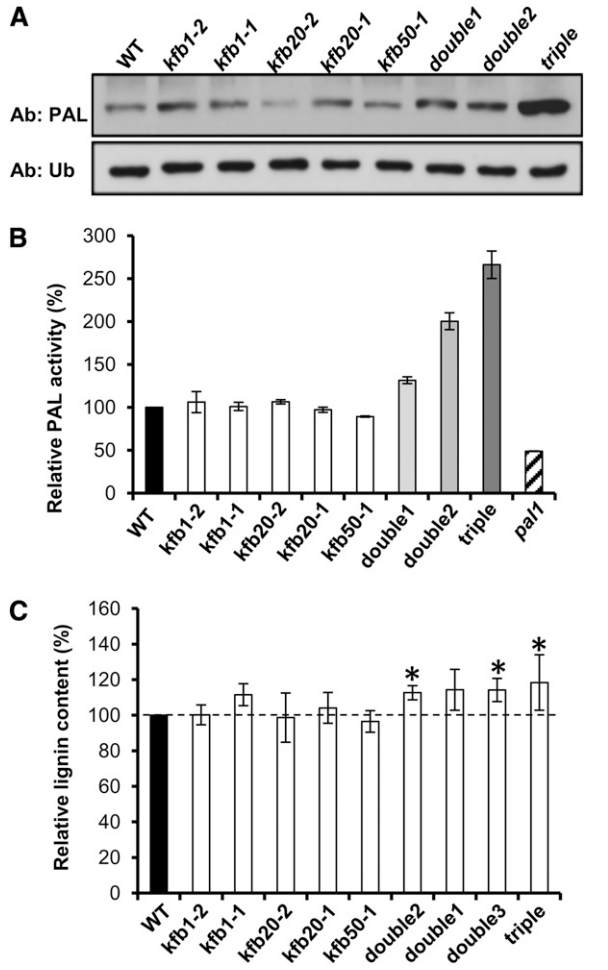

Figure 9. Enhancement of the Stability of PAL and the Alteration of Lignin Content in *kfb* Knockout Mutants.

(A) The level of endogenous PAL protein in the *kfb* single to triple mutant lines. The PAL proteins were monitored using a developed anti-PAL peptide antibody. The monoubiquitin immunoblot against the anti-ubiquitin antibody served for controlling the amount of protein loading. WT, the wild type.

(B) The relative PAL enzyme activities in *kfb* mutant lines. The error bars represent the SD from three biological replicates.

(C) The relative lignin content in inflorescent stem of *kfb* mutant lines. The content of acetyl-bromide lignin was measured from the stem of 12-week-old plants, and the level of the wild type was set as 100%. Data are the means of five to approximately eight biological replicates with standard deviations. *Student's *t* test, $P < 0.05$ (in comparison with the wild type). *kfb1-1*, Salk_000312; *kfb1-2*, Salk_014388; *kfb20-1*, Salk_129095; *kfb20-2*, Salk_008497; *kfb50-1*, Salk_080249; *double 1*, *kfb20-1/kfb50-1*; *double 2*, *kfb20-1/kfb1-1*; *double 3*, *kfb20-1/kfb1-2*; *triple*, *kfb20-1/kfb1-1/kfb50-1*.

Table 1. Levels of Anthocyanins, Flavonols, and Sinapoyl Esters Accumulated in the *Arabidopsis kfb* Double or Triple Mutant Seedlings Five Days after Germination

Lines	Anthocyanins (pmol/g FW)	Total Flavonols (pmol/mg FW)	Sinapoyl Malate (pmol/mg FW)
The wild type	75.6 ± 1.9	286.3 ± 15	1896.5 ± 58.3
kfb20-1/kfb1-1	100 ± 2.3	300.2 ± 23	2749.3 ± 78
kfb20-1/kfb1-2	99.3 ± 1.9	298.1 ± 6.7	2503.4 ± 57.9
kfb20-1/kfb50-1	110.8 ± 1.5	330.6 ± 18	4001.6 ± 95
kfb20-1/kfb1-1/kfb50-1	302.4 ± 13	310.8 ± 19.3	5120.55 ± 109.1

Data are mean values and standard errors from three biological replicates. *kfb1-1*, Salk_000312; *kfb1-2*, Salk_014388; *kfb20-1*, Salk_129095; *kfb20-2*, Salk_008497; *kfb50-1*, Salk_080249. FW, fresh weight.

the overexpression of *KFB* disturbed phenylpropanoid biosynthesis. Subsequently, we undertook more detailed analyses on the selected T2 generation of transgenic lines to validate their inheritance of the KFB-mediated phenotypes; a few phenylpropanoid-lignin biosynthetic mutant lines, including *pal1*, *c4h*, *lac4*/*lac17*, and *tt4* were included as positive controls. qRT-PCR analysis verified the overexpression of three *KFB* transgenes in the selected transgenic lines (Figure 10). Interestingly, in some *KFB* transgenic lines, we observed upregulated transcription of *PAL* isogenes, particularly *PAL1*, *PAL2*, and *PAL3* (Figure 10). This increase in transcription probably reflects positive feedback regulation of *PAL* expression at the mRNA levels in response to its protein turnover (illustrated in Figure 11). However, the intensity of the immunosignals of the PAL proteins was substantially less in crude extracts from the *KFB01*, *KFB20*, and *KFB50* overexpression lines than in the control plants (Figure 11A; see Supplemental Figure 9 online); the decline in stability in general coincided with the more than 50 to ~70% reduction of PAL activity in the T2 transgenic lines (Figure 11B). The decreased level of protein and of the activity of PALs in transgenic plants were not due to the impairment of transcription of the PAL genes, since their transcripts in most independent *KFB* transgenic lines were upregulated, particularly, for the *PAL1*, *PAL2*, *and PAL3* genes (Figure 10).

Disruption of *PAL1* or *C4H* in the general phenylpropanoid pathway caused severe reduction of the accumulation of soluble phenolics (Table 2). The *KFB* transgenic *Arabidopsis* leaves also showed a substantial decline in the amounts of anthocyanins, flavonols, and sinapoyl esters, coincident with the alteration in the stability and activity of PAL in those transgenic plants. In particular, the impairment of accumulation of flavonoids and sinapoyl malate in the KFB01 overexpression lines was more drastic than that in *pal1* mutant line deficient in single *PAL* isogene (Table 2; see Supplemental Figure 10 online). Meanwhile, the brownish pigmentation of seed coats, mainly reflecting the accumulated proanthocyanidins (Xie et al., 2003), had largely faded in the mature seeds of some of *KFB* transgenic lines, a phenotype that was reminiscent of the classic *transparent testa* mutant seeds deficient in flavonoid/anthocyanin biosynthesis (Winkel-Shirley, 2001) (Figure 12A). The violet-red lignin staining pointed to the impairment of lignin deposition either in the interfascicular fibers or the xylem bundles of the basal stem of 6-week-old *KFB* transgenic plants (Figure 12B). Furthermore, we found a decrease of up to 24% in the content of acetyl bromide lignin in the mature stem of selected T2 transgenic plants compared with the level in control plants (Figure 12C). These data suggest that the overexpression of *KFB01*, *KFB20*, and *KFB50* promoted the turnover of endogenous PAL enzymes, thus disturbing phenylpropanoid biosynthesis.

DISCUSSION

As a major branch point between the primary and secondary metabolic pathways in plants, PAL directs up to 30% of the fixed carbon source from the shikimate pathway to different phenolics (Rohde et al., 2004). Its activity is exquisitely regulated during the developmental phases associated with the cell type–specific synthesis of lignin and the flavonoid pigments and by an array of environmental cues associated with generating the phenylpropanoid products involved in adaptation or protection (Dixon and Paiva, 1995). Different mechanisms control the activity of this rate-limiting enzyme (Dixon and Paiva, 1995; Martin and Paz-Ares, 1997; Weisshaar and Jenkins, 1998; Vogt, 2010). For example, in many species and cell suspension cultures, PAL activity was induced transiently in response to biotic or abiotic stimuli. Such transient increases of PAL activity, which often constitute an early defense response leading to accumulation of phenylpropanoid-derived phytoalexins in the cell cultures, was evident as a consequence of a rapid stimulation of *PAL* mRNA

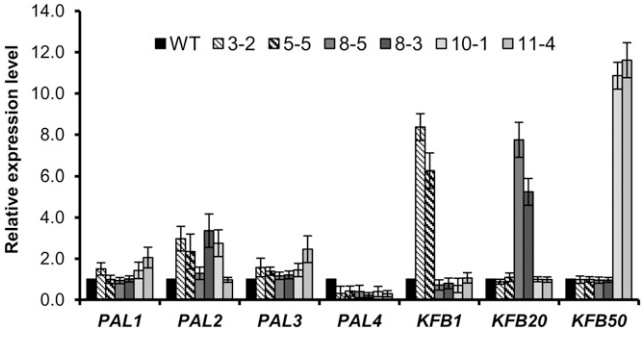

Figure 10. Expression of *KFB* Transgenes and Endogenous *PAL* in the T2 Generation of *KFB* Overexpression *Arabidopsis* Lines.

The expression level detected by qRT-PCR for each gene, after normalization to that of ubiquitin10 control gene, is expressed as a value relative to its level in the wild type (WT). Data are the means of the three replicates with standard deviations. *KFB1* OE lines: 3-2, 5-5; *KFB20* OE lines: 8-5, 8-3; *KFB50* OE lines: 10-1, 11-4.

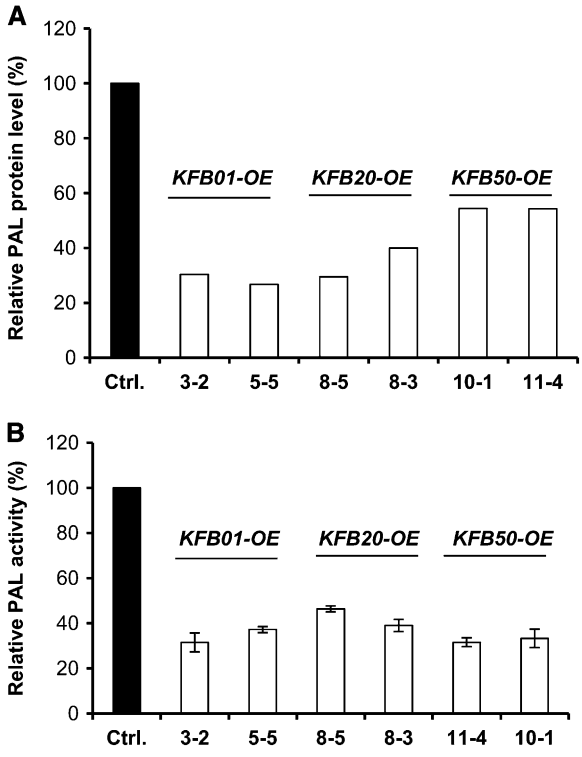

Figure 11. Attenuation of the Stability of PAL by the Overaccumulated KFB in Planta.

(A) Quantification of the level of PAL protein based on the gel blot image, shown in Supplemental Figure 9 online by ImageJ software in the T2 *KFB* overexpression lines of *Arabidopsis*. The amount of PAL proteins from two independent T2 transgenic lines of each *KFB* genes was monitored using a developed anti-PAL peptide antibody and then normalized with the monoubiquitin immunosignal detected against antiubiquitin antibody. **(B)** The relative PAL enzyme activities in *KFB* overexpression transgenic lines. The total PAL activity detected in the control was 10 ± 0.4 pmol/mg/h. The error bars represent the SD from three biological replicates.

synthesis that engenders the de novo synthesis of enzymes (Edwards et al., 1985). The subsequent rapid decay of the induced activity was considered to be a posttranslational event (Tanaka and Uritani, 1977; Lamb et al., 1979; Lawton et al., 1980; Shields et al., 1982; Jones, 1984). Some researchers proposed an inactivation mechanism that reversibly converts PAL to its inactive form (Attridge and Smith, 1973; French and Smith, 1975; Creasy, 1976), but an immunoprecipitation experiment suggested that the decline in PAL activity might be due to its proteolytic turnover (Tanaka and Uritani, 1977). In our study, evidence from in vitro and in planta experiments suggests that a group of ubiquitin E3 ligase F-box proteins specifically interact with PAL isozymes and mediate their degradation through the ubiquitination-26S proteasome pathway.

SCF-Mediated Polyubiquitination and Proteolysis of PAL

The SCF ubiquitin ligase complex affects a variety of developmental processes, phytohormone-mediated signal transduction pathways, and defense responses in plants. The F-box protein subunit imparts specificity for ubiquitinating selected target proteins (del Pozo and Estelle, 2000; Lechner et al., 2006). In contrast with the growing numbers of studies on the involvement of ubiquitin-protein degradation pathway in regulating plant growth, development, and signaling transduction cascades, information is scarce on its role in controlling the plant's secondary metabolism, particularly phenylpropanoid-lignin biosynthesis. Several lines of evidence in the present study revealed that the KFB01, KFB20, and KFB50 proteins, a subclass of F-box proteins, dominate PAL degradation. We affirmed the physical interaction between the individual KFBs and PAL isozymes in a series of complementary biochemical and cellular approaches; these include the genome-wide Y2H screening, followed by the pairwise Y2H validation (Figure 1), the in planta BiFC assays, and the co-IP of KFBs with PAL isozymes (Figures 2 and 3). The bright cytosolic chimeric BiFC signals of the pairs of the truncated KFB- and PAL-half fluorescence proteins in the living cells and the co-IP of nYFP-KFB fusion protein by PAL(s)-CFPc coincide with our observations in the Y2H assay. The observed complementary fluorescent signal in BiFC and the immunodetection of KFB in the co-IP assay are not due to the artificial interaction of the tagged fluorophores, since the nonfunctional fluorophore fragments in general do not reassemble spontaneously and the refolding and reconstitution of a fluorescing protein only occurs at the fused partner proteins tightly interact (Kerppola, 2006, 2008; Gehl et al., 2009). The impossibility of an artificial interaction resulted from spontaneous reassembly of fluorescent fragments was validated further by our inclusion of a similar F-box protein, CPR30, as the negative control in both the BiFC and co-IP assays (Figures 2 and 3; see Supplemental Figure 3 online), where the CPR30 was tagged with fragment of fluorescence protein in a manner similar to the KFBs and coexpressed with the PAL fusion proteins. The combination failed to generate any fluorescence emission in BiFC, and it was not pulled down by PAL fusion in the co-IP (Figures 2 and 3; see Supplemental Figure 3 online), demonstrating the viability of the adopted BiFC and co-IP systems and the specific interaction of the identified KFBs and PAL isozymes.

F-box protein dominates the substrate specificity of SCF ubiquitin ligase, leading to ubiquitylation and degradation of the selected target proteins (del Pozo and Estelle, 2000; Lechner et al., 2006). Indeed, the interaction of PAL and KFB resulted in a discernible attenuation of PAL stability. Coexpression of KFB and PAL substantially diminished PAL concentration and activity (Figure 5). This effect on PAL stability by KFBs was evidenced further by manipulating *KFB* expression in planta (Figures 9 and 11); disrupting or overexpressing the *KFBs* in *Arabidopsis* resulted in a reciprocal fluctuation of the endogenous level of the PAL protein, suggesting that KFBs control PAL stability in living cells. Moreover, we found that the PAL isozymes were (poly) ubiquitylated in vivo (Figure 7). When blotted against the anti-ubiquitin antibody, a ladder of slow-mobility immunobands of the enriched PALs from the infiltrated tobacco leaves pointed to the existence of polyubiquitinated PAL species in vivo (Figure 7). This slow mobility pattern of (poly)ubiquitylated protein species was commonly found in other studies (Shanklin et al., 1987, 1989). Our detection of the polyubiquitylation of the PAL proteins also corresponds with a previous study in globally

Table 2. Levels of Accumulated Anthocyanins, Flavonols, and Sinapoyl Esters in the T2 Generation of *KFB* Overexpression *Arabidopsis* Leaves

Lines	Anthocyanins (pmol/g FW)	Total Flavonols (pmol/mg FW)	Sinapoyl Malate (pmol/mg FW)
Wild type/*pMDC32*	66.9 ± 0.6	315 ± 3	2233 ± 321
c4 h	4.0 ± 0.12	69 ± 4	79.93 ± 11.26
pal1	12.7 ± 0.31	207 ± 14	870 ± 130
tt4	n/a	n/a	3331 ± 479
lac4/17	69.6 ± 0.07	245 ± 36	2390 ± 344
KFB01-OE			
#3-2	21.6 ± 0.6	138 ± 6	290 ± 40
#5-5	51.8 ± 1.8	106 ± 6.4	140 ± 20
KFB20-OE			
#8-5	8.5 ± 0.2	153 ± 21	800 ± 100
#8-3	25.4 ± 0.3	146 ± 16	740 ± 106
KFB50-OE			
#11-4	31.9 ± 0.3	160 ± 18	740 ± 110
#10-1	17.9 ± 0.4	150 ± 10	751 ± 108

Data are mean values and standard deviation from three replicate analyses. n/a, undetectable; FW, fresh weight.

detecting ubiquitylated proteins in *Arabidopsis*, which predicted that PAL is ubiquitylated (Saracco et al., 2009). The ubiquitylation status of PAL was further serendipitously corroborated by LC-MS analyses (see Supplemental Data Set 1 online), although the abundance of the detected Ub peptides is low, probably due to the mass spectrometric approach we adopted that is not optimized for analyzing plant ubiquitylated species (Saracco et al., 2009). Furthermore, the PAL degradation was sensitive to MG132, the specific inhibitor of 26S proteasome (Figure 6), and the ubiquitylated PAL species appeared to be stabilized by this proteasome inhibitor (Figure 7). Collectively, all these in vitro and in vivo data suggest PAL is degraded via the ubiquitination-26S proteasome pathway, in which the identified KFBs are the key determinants for PAL proteolytic turnover.

Biological Implication of KFB-Mediated PAL Degradation

The ubquitination-26S mediated proteolysis has been associated with two basic physiological roles protein recycling by removing abnormal proteins and maintaining the supply of free amino acids during growth and starvation and cellular regulation by removing rate-limiting enzymes and/or regulatory proteins, therefore fine-tuning metabolic homeostasis, facilitating adaptation to changing environments, and programming growth and development (Vierstra, 1996, 2009; Hellmann and Estelle, 2002). Accordingly, one envisioned role of the observed KFB-mediated irreversible proteolysis of PAL might be as a housekeeping mechanism to remove abnormal or unnecessary PAL proteins during metabolism.

However, *KFB*s exhibited preferential expression in different tissues, and their transcription was altered along with the development of the inflorescence stem (Figures 8A and 8B). Most particularly, *KFB20*, the one predominantly expressed in *Arabidopsis* stems and leaves, showed a higher transcript level in the developing node than in basal nodes, where its vasculature was less lignified than was the basal stem (Ehlting et al., 2005). Thus, it appears that the expression of KFB negatively coordinate the developmental activation of phenylpropanoid synthesis and plant lignification.

Furthermore, environmental stimuli also modulate the expression of *KFB*. Treating the carbon-deprived *Arabidopsis* seedlings with exogenous carbon sharply downregulated the expression of *KFB20* and *KFB50* (Osuna et al., 2007). We verified the responses of *KFB* to the rich carbon source or sugar signal in present study. The expression levels of all three *KFB* genes in the seedlings incubated in media containing 4% Suc decreased threefold to ~10-fold compared with plants growing in media containing 1% Suc (Figure 8C). Conversely, PAL concentration increased substantially and so did the accumulation level of anthocyanins in the seedlings growing on the media containing more sugar (see Supplemental Figure 5 online). This is consistent with the previous reports that the high carbon source or the related sugar signaling induces flavonoid/anthocyanin accumulation as well as lignin deposition (Rogers et al., 2005; Solfanelli et al., 2006). The decreased expression of *KFBs* in an environment rich in carbon affects the activation of phenylpropanoid biosynthesis by mitigating the turnover of the rate-limiting enzyme, PAL, which suggest that *KFBs* are coordinately regulated to modulate phenylpropanoid biosynthesis. Also, treating *Arabidopsis* seedlings with nitrogen upregulated the expression of *KFB20* (Scheible et al., 2004). PAL activity links carbon sequestration and nitrogen assimilation; the deamination reaction of PAL liberates an ammonium group, which then is assimilated, via Gln synthase, into carbon skeletons (Singh et al., 1998). Crosstalk between the nitrate level and phenylpropanoid metabolism was demonstrated in tobacco (Fritz et al., 2006), where PAL functions critically in maintaining the proper ratio of carbon:nitrogen. The induction of *KFB* gene expression by N_2 might link to the exquisite control of PAL stability, and thus activity, thereby regulating the nitrogen assimilation and carbon sequestration to phenylpropanoids. These data corroborate a negative correlation of *KFB* gene expression and phenylpropanoid accumulation.

Finally, genetically manipulating the expression of *KFBs* (by gene disruption or overexpression) reciprocally affects the accumulation of a broad array of soluble phenolics, including UV-protectant hydroxycinnamate esters, flavonoid/anthocyanin pigments, and the cell wall structural component, lignin (Figures

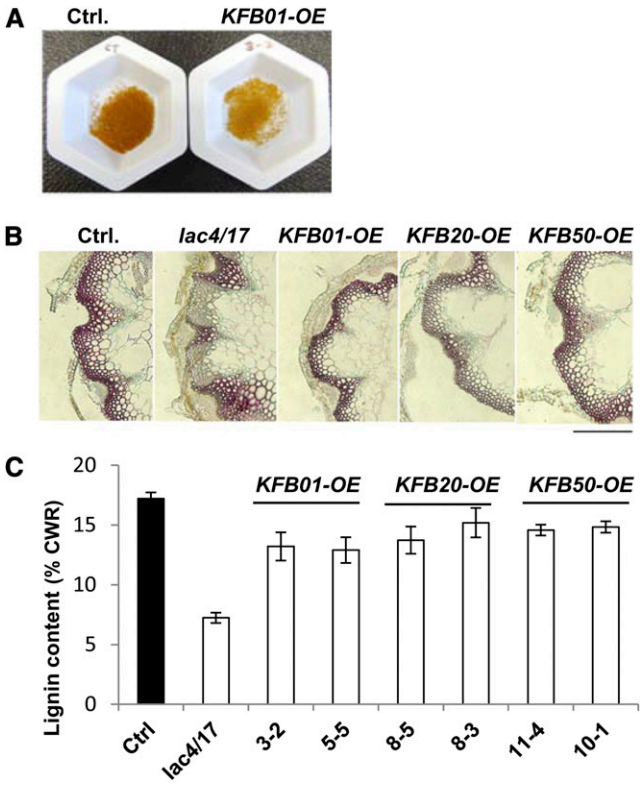

Figure 12. Overexpression of *KFB* Genes Impairs Phenylpropanoid-Lignin Synthesis.

(A) The change in seed coat pigmentation of a KFB transgenic line.
(B) Phloroglucinol staining of total lignin in *KFB* overexpression transgenic *Arabidopsis* showing one representative T2 line for each *KFB* transgenes. The plants harboring an empty vector and the lignification-deficient mutant *lac4 lac17* served as the controls. Bar = 300μm.
(C) Total lignin content in *KFB* overexpression transgenic *Arabidopsis*. Two representative independent T2 lines for each transgene were measured for the acetyl bromide lignin. CWR, cell wall residue.

9 and 12, Tables 1 and 2). This genetic and metabolic evidence indicates that the KFB-mediated turnover of PAL might not (or not only) act in removing or recycling abnormal PAL proteins in the metabolic process, but also, as a basic posttranslational modification mechanism, participate in programming carbon flux toward phenylpropanoid metabolites by controlling the stability of this rate-limiting enzyme. Other recently published work found that the same group of KFB proteins (which they denoted KISS ME DEADLY) also physically interact with a few regulators of the cytokinin response, the type-B *Arabidopsis* response regulators, for degradation, thus negatively regulating the responses of *Arabidopsis* to cytokinin signals (Kim et al., 2013). The cytokinin signaling cascade has a central role in regulating cell division; it also modulates the development of the shoots and roots and stress responses (Sakakibara, 2006). F-box proteins can selectively target a set of substrates (Craig and Tyers, 1999; del Pozo and Estelle, 2000; Gagne et al., 2002; Risseeuw et al., 2003; Ho et al., 2008). The alteration of phenylpropanoid-lignin biosynthesis, along with the disturbance of *KFB* gene expression, is unlikely attributable to the changes in *Arabidopsis* response regulator stability and the cytokinin response, since, for example, the reduction of the levels of phenolics and lignin in the *KFB* overexpression lines is not due to the downregulation of *PAL* transcription but to the decrease in enzyme concentration (Figures 10 and 11). Considering the possibility of multiple targets of the identified KFBs, this group of proteins may act as the key regulatory linkers in planta by mediating the selective degradation of both catalytic enzymes and regulatory proteins, physiologically and metabolically coordinating the hormonal-signaling cascade and phenylpropanoid biosynthesis. It will be interesting to systematically explore the comprehensive set of the specific targets of KFBs and their potential roles in coordinating different biological and metabolic processes.

In summary, our in vitro and in vivo biochemical and genetic evidence demonstrated that *Arabidopsis* PAL isozymes are subjected to degradation via the SCF type of E3 ubiquitin ligase-mediated ubiquitination-26S proteasome system, wherein the Kelch repeat F-box proteins act as the key mediators, specifying the turnover of the targeted PAL isoforms. This posttranslational modification can substantially affect phenylpropanoid biosynthesis and plant lignification. As many phenylpropanoids, such as anthocyanins, flavonoids, and phenolic esters, are bioactive chemicals with potential health-promoting activity to plants and humans, the identification and characterization of these posttranslational regulators of the rate-limiting enzymes offer additional tools for modulating their production.

METHODS

Y2H Assay

The full-length cDNAs of *Arabidopsis thaliana* PAL1-4 were isolated by RT-PCR using the primers described in Supplemental Table 1 online and cloned into the bait vector pGBKT7 (Clontech). *Arabidopsis*-normalized cDNA expression library in Y187 yeast cells, in which cDNAs were ligated in the prey vector pGADT7-RecAB, was purchased from Clontech. The Y2H screen and the pairwise verification were performed according to the manufacturer's instructions (Clontech).

Transient Expression of PAL in Tobacco Leaves and Cell-Free Degradation Assay

The native or tagged versions of the PALs and KFB proteins were expressed transiently in tobacco (*Nicotiana tabacum*) leaves following the procedures of Sparkes et al. (2006).

For the cell-free degradation assay, the crude proteins were extracted from the *PAL-GFP* transient expression tobacco leaves using 50 mM Tris-HCl buffer, pH 7.5, containing 150 mM NaCl, 10 mM MgCl, 1 mM EDTA, 10% glycerol, 0.1% Nonidet P-40, and a 1× 13 complete Roche protease inhibitor cocktail. The PAL(s)-GFP proteins were enriched from the tobacco leaves via the Chromotek-GFP Trap following the manufacturer's instructions (Allele). The enriched PAL(s)-GFP protein was incubated at 30°C with the crude proteins that were extracted from 6-week-old *Arabidopsis* stem tissues with 25 mM Tris-HCl buffer, pH 7.5, containing 10 mM NaCl, 10 mM $MgCl_2$, 4 mM phenylmethylsulfonyl fluoride, 5 mM DTT, and 10 mM ATP, and then they were sampled at the intervals stated. The abundance of the remaining PAL(s)-GFP proteins in the samples was determined by immunoblotting against the anti-GFP antibody. For treatments with the proteasome inhibitor, 0.4 mM MG132 was incubated with *Arabidopsis* crude protein extracts for 20 min before conducting the cell-free degradation assay.

BiFC Assay

To generate the BiFC constructs, we subcloned the full-length *PAL1-4* genes, the full-length or truncated *KFB* genes, and the truncated CPR30 gene into the p(MAS)DEST-GW SCYCE, p(MAS)DEST-GW SCYCE (R), pDEST-GW VYNE(R), pDEST-GW VYNE, or pDEST-GW VYNE(R) vectors accordingly (Gehl et al., 2009) from their entry vectors. The coexpression was conducted in 4- to 6-week-old tobacco leaves as described (Gehl et al., 2009). The chimeric fluorescence of the expressed fusion proteins was detected 2 to 4 d after infiltration. Fluorescence images were captured via a Leica TCS SP5 laser scan confocal microscope with excitation at 488 and 496 nm and an emission wavelength between 507 and 549 nm for nYFP-CFPc chimeric signals and 636 and 725nm for chloroplast autofluorescence signals.

Co-IP

Tobacco leaves transiently singly expressing or coexpressing PAL(s)-HA-CFPc fusion protein (~100 kD) and the individual nYFP-Myc-KFB(ΔF) proteins were harvested 2 to ~4 d after infiltration. We extracted the total soluble proteins from homogenized tobacco leaves with a 50 mM Tris-HCl buffer, pH 7.5, containing 2 mM EDTA, 150 mM NaCl, 10% glycerol, 5 mM DTT, 0.25% Triton-X 100, and 1× complete protease inhibitor cocktail. To precipitate the antibody-antigen complexes, we mixed 20 μL of Red Anti-HA Affinity gel beads (Sigma-Aldrich) with the crude protein extracts and agitated them overnight at 4°C. The affinity beads then were pelleted by centrifugation for 1 min at 1000*g* and washed three times with 1 mL of immunoprecipitation buffer (25 mM Tris-HCl, pH 7.5, 1 mM EDTA, 150 mM NaCl, 0.15% Nonidet P-40, and 1× protease inhibitor cocktail). The protein-bound beads were mixed with 50 μL of the SDS-PAGE sample buffer and incubated at 42°C or boiled for 10 min, and 10-μL immunoprecipitated samples were separated by SDS-PAGE gel. Immunoblot analyses were performed according to the ECL Western Blotting procedure (GE Healthcare) using monoclonal anti-HA antibody, HAII clone 16B12 (Covance), or monoclonal anti-c-Myc antibody (9E10: sc-40; Santa Cruz).

For the LC-MS analysis, the PAL1-HA-CFPc protein was immunoprecipitated with anti-HA antibody and then developed on SDS-PAGE gel. After staining with Coomassie Brilliant Blue R 250, the visible double bands from the sample of PAL1-HA-CFPc and nYFP-Myc-KFB50 (ΔF) coinfiltration were cut out. The gel slices then were reduced and alkylated sequentially with DTT and iodoacetamide. After trypsin digestion, the samples were subjected to LC-MS analysis.

In Vivo Ubiquitination Analysis

Tobacco leaves first were infiltrated with 35S:PAL(s)-HA cassette (in pGWB414). Three days after the first infiltration, each half leaf was pre-infiltrated with infiltration buffer with or without 40 μM MG132 and left for 5 h before sampling. One gram of leaf tissues from each sample was homogenized in a protein extraction buffer as described above. To examine the ubiquitylation of PAL(s)-HA, the crude protein extracts were incubated with 20 μL of Red Anti-HA Affinity gel beads (Sigma-Aldrich) and then washed three times extensively with immunoprecipitation buffer, as described above. The protein-bound beads were mixed with 50 μL of SDS-PAGE sample buffer and incubated at room temperature, 42, 60, or 100°C for 10 min, and 10-μL IPed samples were separated by SDS-PAGE gel. Both anti-HA (Covance) and antiubiquitin (Agrisera) antibodies were used for the immunoblot.

Arabidopsis Growth Conditions and qRT-PCR Analysis

Arabidopsis seeds were surface-sterilized with 10% (v/v) bleach for 10 min and washed three times with 0.1% Triton X-100 water. Sterilized seeds were plated on a one-half-strength Murashige and Skoog medium containing 0.8% agar and 1% Suc. For treating with a high-carbon source, the medium contained 4% Suc. Seeds were stratified at 4°C for 2 to ~3 d and then germinated under continuous light at 22°C. Seven-day-old seedlings were transferred into soil and grown under photoperiodic cycles of 16 h of light and 8 h of dark at 22°C in a growth chamber.

For qRT-PCR analysis, the total RNAs were isolated using the RNeasy plant mini kit (Qiagen Sciences) from the tissues of rosette leaves, cauline leaves, stems, flowers, and buds, young siliques of 6-week-old plants, and the separated stem nodes from the bottom to top. cDNAs were obtained using Moloney Murine Leukemia Virus reverse transcriptase (Promega). We treated these RNA samples with DNase I (New England Biolabs) following the manufacturer's protocol. Reverse transcription reactions were performed by employing the Moloney Murine Leukemia Virus reverse transcriptase (Promega). For quantitative PCR analysis, the reaction was set with SsoAdvanced SYBR Supermix (Bio-Rad) following the formalized standard procedure described by Udvardi et al. (2008). The delta cycle threshold method was used to quantify individual gene expression, and the *Arabidopsis* Ubiquitin10 (At4g05320) gene was used as the control for normalization.

Identifying and Generating *kfb* Homozygous Mutant Lines

The T-DNA insertion mutant lines of Salk_000312 and Salk_014388 for At1g15670 (*KFB01*), Salk_129095 and Salk_008497 for At1g80440 (*KFB20*), and Salk_080249 for At3g59940 (*KFB50*) were obtained from the ABRC; the T-DNA insertions were confirmed by genomic PCR, and the transcripts of the disrupted genes were examined by RT-PCR using the primers listed in the Supplemental Table 1 online. The homozygous mutant alleles deficient in the single *KFB* gene were crossed and the F2 cross-progenies were selected by PCR; the absence of the *KFB* transcripts was confirmed by RT-PCR using RNAs extracted from F3 populations of the double or triple mutant seedlings 5 d after germination. For soluble phenolic extraction, 4-week-old plants were used, and for lignin measurement, mature stems of 12 weeks were used.

Generating *KFB* Transgenic Plants and Examining PAL Activity and Stability

Full-length *KFB* cDNAs were subcloned into binary vector pMDC32 (Curtis and Grossniklaus, 2003) and transferred into *Arabidopsis* (Columbia-0) by the floral dip method (Clough and Bent, 1998). To measure the PAL enzyme activity of the F-box protein transgenic plants, the crude proteins were extracted from 4-week-old whole plants of the T2 generation lines. The enzymatic assays were performed following the protocol described (Edwards and Kessmann, 1992). To examine the protein levels of endogenous PALs in transgenic lines, we synthesized peptides C-MDPLQKPKQDRYALR and used them to raise the anti-PAL antibody (Pacific Immunology) that we then employed in the immunoblot analyses.

Analyses of Soluble and Cell Wall Phenolics

Flavonoids and soluble phenolics were extracted from 4-week-old T2 plants and analyzed by LC-MS as described by Zhang et al. (2012). Anthocyanin was extracted overnight from the seedlings of 4-week-old T2 plants with 1% HCl (v/v) in 80% methanol at 4°C. The extracts were collected. For measuring the anthocyanin content, we employed a spectroscopic method. Briefly, we determined the appropriate dilution factor for the samples by diluting the methanolic extracts with 25 mM KCl buffer, pH 1.0, until the absorbance of the sample at the 510 nm fell within the linear range of the spectrophotometer. Then, based on this factor, we prepared two dilutions of the samples, one with 25 mM KCl buffer, pH 1.0, and the other with 0.4 M sodium acetate buffer, pH 4.5. These dilutions were equilibrated for 15 min before we measured the absorbance of each dilution at 510 nm and at 700 nm (to correct for haze) against a blank cell

filled with distilled water. The absorbance of the diluted sample (A) was calculated as follows: A = (A_{510} to A_{700}) at pH 1.0 – (A_{510} to A_{700}) at pH 4.5. The concentration of monomeric anthocyanin pigment in the original sample was calculated using the following formula: anthocyanin pigment (mg/L) = (A × MW × DF × 1000)/(ε×1), where MW is the molecular weight of cyandindin-3-glucoside (449.2), DF is the dilution factor, and ε is the molar absorptivity of cyanindin-3-glucoside (26,900).

Lignin was analyzed histochemically using 15-μm-thick cross sections from the first basal node of the 6-week-old stems following standard protocols using 1% phloroglucinol (Wiesner). The acetyl-bromide lignin was measured using the mature inflorescence stems of both wild-type and transgenic plants after 3 months of growth as described (Zhang et al., 2012).

Accession Numbers

Sequence data from this article can be found in the Arabidopsis Genome Initiative or GenBank/EMBL databases under the following accession numbers: At1g15670 (KFB01), At1g80440 (KFB20), At3g59940 (KFB50), At2g37040 (PAL1), At3g53260 (PAL2), At5g04230 (PAL3), At3g10340 (PAL4), and At4g05320 (Ubiquitin10).

Supplemental Data

The following materials are available in the online version of this article.

Supplemental Figure 1. Detected KFB Prey Proteins in the Initial Y2H Screening Using *Arabidopsis* PAL2 as the Bait.

Supplemental Figure 2. Subcellular Localization of PAL- and KFB-GFP Fusion Proteins Transiently Expressed in Tobacco Epidermal Cells.

Supplemental Figure 3. Negative Control for Co-IP Experiments of PAL–KFB Interaction.

Supplemental Figure 4. Effect of the Preparation Conditions on the Stability of Immunoprecipitated PAL-HA Protein.

Supplemental Figure 5. Effect of Exogenous Suc Supply on PAL's Transcription, Total PAL Protein Concentration, and the Content of Accumulated Anthocyanin.

Supplemental Figure 6. Characterization of the *kfb* T-DNA Insertion Mutant Lines.

Supplemental Figure 7. The Relative PAL Activity and Lignin Content in the Cell Walls of the T1 Generation of the *KFB01*, *KFB20*, and *KFB50* Overexpression Lines of *Arabidopsis*.

Supplemental Figure 8. Effect of *KFB* Overexpression on Anthocyanin Pigmentation in T1 Transgenic Lines.

Supplemental Figure 9. Gel Blotting Analysis on the Level of Endogenous PAL Protein in the *KFB* Overexpression Transgenic *Arabidopsis*.

Supplemental Figure 10. UV-HPLC Profiles of Soluble Phenolics in *KFB01* Overexpression Line (#3-2) Compared with the Control (Wt/pMDC32), *pal1*, *c4h*, and *tt4* Mutants.

Supplemental Table 1. Primers Used in the Study.

Supplemental Data Set 1. LC-MS Analysis on the Immunoprecipitated PAL-HA-CFPc Doublet Proteins.

ACKNOWLEDGMENTS

We thank Lise Jouanina (Institut Jean Pierre Bourgin, France) for sharing *Lac4/17* double mutant seeds and John Shanklin (Brookhaven National Laboratory, USA) for discussing protein ubiquitylation with us. This work is supported by the Division of Chemical Sciences, Geosciences, and Biosciences, Office of Basic Energy Sciences of the U.S. Department of Energy through Grant DEAC0298CH10886 (BO-147 and 157) to C.-J.L. The use of the confocal microscope in the Center for Nanosciences was supported by the Office of Basic Energy Sciences, U.S. Department of Energy, under Contract DEAC02-98CH10886.

AUTHOR CONTRIBUTIONS

X.Z., M.G., and C.-J.L. designed the experiments. X.Z. performed theY2H assays, protein subcellular localization, and cell-free assay and generated and analyzed transgenic plants. M.G. conducted BiFC and co-IP and detected the ubiquitylation of the PAL isozymes. X.Z. and C.-J.L. wrote the article. All authors discussed the results and edited the article.

Received October 14, 2013; revised November 14, 2013; accepted December 3, 2013; published December 20, 2013.

REFERENCES

Achnine, L., Blancaflor, E.B., Rasmussen, S., and Dixon, R.A. (2004). Colocalization of *L*-phenylalanine ammonia-lyase and cinnamate 4-hydroxylase for metabolic channeling in phenylpropanoid biosynthesis. Plant Cell **16:** 3098–3109.

Arabidopsis Interactome Mapping Consortium (2011). Evidence for network evolution in an *Arabidopsis* interactome map. Science **333:** 601–607.

Attridge, T.H., and Smith, H. (1973). Evidence for a pool of inactive phenylalanine ammonia-lyase in *Cucumis sativus* seedlings. Phytochemistry **12:** 1569–1574.

Bassard, J.E., Mutterer, J., Duval, F., and Werck-Reichhart, D. (2012). A novel method for monitoring the localization of cytochromes P450 and other endoplasmic reticulum membrane associated proteins: a tool for investigating the formation of metabolons. FEBS J. **279:** 1576–1583.

Bate, N.J., Orr, J., Ni, W., Meromi, A., Nadler-Hassar, T., Doerner, P.W., Dixon, R.A., Lamb, C.J., and Elkind, Y. (1994). Quantitative relationship between phenylalanine ammonia-lyase levels and phenylpropanoid accumulation in transgenic tobacco identifies a rate-determining step in natural product synthesis. Proc. Natl. Acad. Sci. USA **91:** 7608–7612.

Bolwell, G.P., Bell, J.N., Cramer, C.L., Schuch, W., Lamb, C.J., and Dixon, R.A. (1985). *L*-Phenylalanine ammonia-lyase from *Phaseolus vulgaris*. Characterisation and differential induction of multiple forms from elicitor-treated cell suspension cultures. Eur. J. Biochem. **149:** 411–419.

Bork, P., and Doolittle, R.F. (1994). Drosophila kelch motif is derived from a common enzyme fold. J. Mol. Biol. **236:** 1277–1282.

Boudet, A.M. (2007). Evolution and current status of research in phenolic compounds. Phytochemistry **68:** 2722–2735.

Broun, P. (2005). Transcriptional control of flavonoid biosynthesis: A complex network of conserved regulators involved in multiple aspects of differentiation in *Arabidopsis*. Curr. Opin. Plant Biol. **8:** 272–279.

Bubna, G.A., Lima, R.B., Zanardo, D.Y., Dos Santos, W.D., Ferrarese, Mde.L., and Ferrarese-Filho, O. (2011). Exogenous caffeic acid inhibits the growth and enhances the lignification of the roots of soybean (*Glycine max*). J. Plant Physiol. **168:** 1627–1633.

Clough, S.J., and Bent, A.F. (1998). Floral dip: A simplified method for *Agrobacterium*-mediated transformation of *Arabidopsis thaliana*. Plant J. **16:** 735–743.

Cochrane, F.C., Davin, L.B., and Lewis, N.G. (2004). The *Arabidopsis* phenylalanine ammonia lyase gene family: Kinetic characterization of the four PAL isoforms. Phytochemistry **65:** 1557–1564.

Craig, K.L., and Tyers, M. (1999). The F-box: A new motif for ubiquitin dependent proteolysis in cell cycle regulation and signal transduction. Prog. Biophys. Mol. Biol. **72:** 299–328.

Cramer, C.L., Edwards, K., Dron, M., Liang, X., Dildine, S.L., Bolwell, G.P., Dixon, R.A., Lamb, C.J., and Schuch, W. (1989). Phenylalanine ammonia-lyase gene organization and structure. Plant Mol. Biol. **12:** 367–383.

Creasy, L.L. (1976). Phenylalanin ammonia-lyase inacctivating system in sunflower leaves. Phytochemistry **15:** 673–675.

Curtis, M.D., and Grossniklaus, U. (2003). A Gateway cloning vector set for high-throughput functional analysis of genes in planta. Plant Physiol. **133:** 462–469.

del Pozo, J.C., and Estelle, M. (2000). F-box proteins and protein degradation: An emerging theme in cellular regulation. Plant Mol. Biol. **44:** 123–128.

Dixon, R.A., and Paiva, N.L. (1995). Stress-induced phenylpropanoid metabolism. Plant Cell **7:** 1085–1097.

Edwards, K., Cramer, C.L., Bolwell, G.P., Dixon, R.A., Schuch, W., and Lamb, C.J. (1985). Rapid transient induction of phenylalanine ammonia-lyase mRNA in elicitor-treated bean cells. Proc. Natl. Acad. Sci. USA **82:** 6731–6735.

Edwards, R., and Kessmann, H. (1992). Isoflavonoid phytoalexins and their biosynthetic enzymes. In Molecular Plant Pathology: A Practical Approach, S.J. Gurr, M.J. McPherson, and D.J. Bowles, eds (Oxford, UK: IRL Press), pp. 45–62.

Ehlting, J., et al. (2005). Global transcript profiling of primary stems from *Arabidopsis thaliana* identifies candidate genes for missing links in lignin biosynthesis and transcriptional regulators of fiber differentiation. Plant J. **42:** 618–640.

Fraser, C.M., and Chapple, C. (2011). The phenylpropanoid pathway in *Arabidopsis*. The Arabidopsis Book **9:** e0152, doi/10.1199/tab.0152.

French, C.J., and Smith, H. (1975). An inactivator of phenylalanine ammonia-lyase from Gherkin hypocotyls. Phytochemistry **14:** 963–966.

Fritz, C., Palacios-Rojas, N., Feil, R., and Stitt, M. (2006). Regulation of secondary metabolism by the carbon-nitrogen status in tobacco: Nitrate inhibits large sectors of phenylpropanoid metabolism. Plant J. **46:** 533–548.

Gagne, J.M., Downes, B.P., Shiu, S.H., Durski, A.M., and Vierstra, R.D. (2002). The F-box subunit of the SCF E3 complex is encoded by a diverse superfamily of genes in *Arabidopsis*. Proc. Natl. Acad. Sci. USA **99:** 11519–11524.

Gehl, C., Waadt, R., Kudla, J., Mendel, R.R., and Hänsch, R. (2009). New Gateway vectors for high throughput analyses of protein-protein interactions by bimolecular fluorescence complementation. Mol. Plant **2:** 1051–1058.

Gou, M., Su, N., Zheng, J., Huai, J., Wu, G., Zhao, J., He, J., Tang, D., Yang, S., and Wang, G. (2009). An F-box gene, CPR30, functions as a negative regulator of the defense response in *Arabidopsis*. Plant J. **60:** 757–770.

Han, L., Mason, M., Risseeuw, E.P., Crosby, W.L., and Somers, D.E. (2004). Formation of an SCF(ZTL) complex is required for proper regulation of circadian timing. Plant J. **40:** 291–301.

Hellmann, H., and Estelle, M. (2002). Plant development: Regulation by protein degradation. Science **297:** 793–797.

Ho, M.S., Ou, C., Chan, Y.R., Chien, C.T., and Pi, H. (2008). The utility F-box for protein destruction. Cell. Mol. Life Sci. **65:** 1977–2000.

Huang, J., Gu, M., Lai, Z., Fan, B., Shi, K., Zhou, Y.H., Yu, J.Q., and Chen, Z. (2010). Functional analysis of the Arabidopsis PAL gene family in plant growth, development, and response to environmental stress. Plant Physiol. **153:** 1526–1538.

Imaizumi, T., Schultz, T.F., Harmon, F.G., Ho, L.A., and Kay, S.A. (2005). FKF1 F-box protein mediates cyclic degradation of a repressor of CONSTANS in *Arabidopsis*. Science **309:** 293–297.

Jones, D.H. (1984). Phenylalanine ammonia-lyase: Regulation of its induction, and its role in plant development. Phytochemistry **23:** 1349–1359.

Kerppola, T.K. (2006). Visualization of molecular interactions by fluorescence complementation. Nat. Rev. Mol. Cell Biol. **7:** 449–456.

Kerppola, T.K. (2008). Bimolecular fluorescence complementation (BiFC) analysis as a probe of protein interactions in living cells. Annu. Rev. Biophys. **37:** 465–487.

Kim, H.J., Chiang, Y.H., Kieber, J.J., and Schaller, G.E. (2013). SCF (KMD) controls cytokinin signaling by regulating the degradation of type-B response regulators. Proc. Natl. Acad. Sci. USA **110:** 10028–10033.

Lamb, C.J., Merritt, T.K., and Butt, V.S. (1979). Synthesis and removal of phenylalanine ammonia-lyase activity in illuminated discs of potato tuber parenchyme. Biochim. Biophys. Acta **582:** 196–212.

Lawton, M.A., Dixon, R.A., and Lamb, C.J. (1980). Elicitor modulation of the turnover of L-phenylalanine ammonia-lyase in French bean cell suspension cultures. Biochim. Biophys. Acta **633:** 162–175.

Lechner, E., Achard, P., Vansiri, A., Potuschak, T., and Genschik, P. (2006). F-box proteins everywhere. Curr. Opin. Plant Biol. **9:** 631–638.

Martin, C. (2013). The interface between plant metabolic engineering and human health. Curr. Opin. Biotechnol. **24:** 344–353.

Martin, C., and Paz-Ares, J. (1997). MYB transcription factors in plants. Trends Genet. **13:** 67–73.

Nelson, D.C., Lasswell, J., Rogg, L.E., Cohen, M.A., and Bartel, B. (2000). FKF1, a clock-controlled gene that regulates the transition to flowering in *Arabidopsis*. Cell **101:** 331–340.

Osuna, D., Usadel, B., Morcuende, R., Gibon, Y., Bläsing, O.E., Höhne, M., Günter, M., Kamlage, B., Trethewey, R., Scheible, W. R., and Stitt, M. (2007). Temporal responses of transcripts, enzyme activities and metabolites after adding sucrose to carbon-deprived *Arabidopsis* seedlings. Plant J. **49:** 463–491.

Raes, J., Rohde, A., Christensen, J.H., Van de Peer, Y., and Boerjan, W. (2003). Genome-wide characterization of the lignification toolbox in Arabidopsis. Plant Physiol. **133:** 1051–1071.

Risseeuw, E.P., Daskalchuk, T.E., Banks, T.W., Liu, E., Cotelesage, J., Hellmann, H., Estelle, M., Somers, D.E., and Crosby, W.L. (2003). Protein interaction analysis of SCF ubiquitin E3 ligase subunits from *Arabidopsis*. Plant J. **34:** 753–767.

Rogers, L.A., Dubos, C., Cullis, I.F., Surman, C., Poole, M., Willment, J., Mansfield, S.D., and Campbell, M.M. (2005). Light, the circadian clock, and sugar perception in the control of lignin biosynthesis. J. Exp. Bot. **56:** 1651–1663.

Rohde, A., et al. (2004). Molecular phenotyping of the pal1 and pal2 mutants of *Arabidopsis thaliana* reveals far-reaching consequences on phenylpropanoid, amino acid, and carbohydrate metabolism. Plant Cell **16:** 2749–2771.

Sakakibara, H. (2006). Cytokinins: Activity, biosynthesis, and translocation. Annu. Rev. Plant Biol. **57:** 431–449.

Saracco, S.A., Hansson, M., Scalf, M., Walker, J.M., Smith, L.M., and Vierstra, R.D. (2009). Tandem affinity purification and mass

spectrometric analysis of ubiquitylated proteins in *Arabidopsis*. Plant J. **59:** 344–358.

Scheible, W.R., Morcuende, R., Czechowski, T., Fritz, C., Osuna, D., Palacios-Rojas, N., Schindelasch, D., Thimm, O., Udvardi, M.K., and Stitt, M. (2004). Genome-wide reprogramming of primary and secondary metabolism, protein synthesis, cellular growth processes, and the regulatory infrastructure of Arabidopsis in response to nitrogen. Plant Physiol. **136:** 2483–2499.

Shanklin, J., Jabben, M., and Vierstra, R.D. (1987). Red light-induced formation of ubiquitin-phytochrome conjugates: Identification of possible intermediates of phytochrome degradation. Proc. Natl. Acad. Sci. USA **84:** 359–363.

Shanklin, J., Jabben, M., and Vierstra, R.D. (1989). Partial purification and peptide mapping of ubiquitin-phytochrome conjugates from oat. Biochem. **28:** 6028–6034.

Shields, S.E., Wingate, V.P., and Lamb, C.J. (1982). Dual control of phenylalanine ammonia-lyase production and removal by its product cinnamic acid. Eur. J. Biochem. **123:** 389–395.

Singh, S., Lewis, N.G., and Towers, G.H. (1998). Nitrogen recycling during phenylpropanoid metabolism in sweet potato tubers. J. Plant Physiol. **153:** 316–323.

Smalle, J., and Vierstra, R.D. (2004). The ubiquitin 26S proteasome proteolytic pathway. Annu. Rev. Plant Biol. **55:** 555–590.

Solfanelli, C., Poggi, A., Loreti, E., Alpi, A., and Perata, P. (2006). Sucrose-specific induction of the anthocyanin biosynthetic pathway in Arabidopsis. Plant Physiol. **140:** 637–646.

Somers, D.E., Kim, W.Y., and Geng, R. (2004). The F-box protein ZEITLUPE confers dosage-dependent control on the circadian clock, photomorphogenesis, and flowering time. Plant Cell **16:** 769–782.

Sparkes, I.A., Runions, J., Kearns, A., and Hawes, C. (2006). Rapid, transient expression of fluorescent fusion proteins in tobacco plants and generation of stably transformed plants. Nat. Protoc. **1:** 2019–2025.

Sun, Y., Zhou, X., and Ma, H. (2007). Genome-wide analysis of Kelch repeat containing F-box family. J. Integr. Plant Biol. **49:** 940–952.

Tanaka, Y., and Uritani, I. (1977). Synthesis and turnover of phenylalanine ammonia-lyase in root tissue of sweet potato injured by cutting. Eur. J. Biochem. **73:** 255–260.

Udvardi, M.K., Czechowski, T., and Scheible, W.R. (2008). Eleven golden rules of quantitative RT-PCR. Plant Cell **20:** 1736–1737.

Vierstra, R.D. (1996). Proteolysis in plants: mechanisms and functions. Plant Mol. Biol. **32:** 275–302.

Vierstra, R.D. (2009). The ubiquitin-26S proteasome system at the nexus of plant biology. Nat. Rev. Mol. Cell Biol. **10:** 385–397.

Vogt, T. (2010). Phenylpropanoid biosynthesis. Mol. Plant **3:** 2–20.

Wanner, L.A., Li, G., Ware, D., Somssich, I.E., and Davis, K.R. (1995). The phenylalanine ammonia-lyase gene family in *Arabidopsis thaliana*. Plant Mol. Biol. **27:** 327–338.

Weisshaar, B., and Jenkins, G.I. (1998). Phenylpropanoid biosynthesis and its regulation. Curr. Opin. Plant Biol. **1:** 251–257.

Winkel-Shirley, B. (2001). Flavonoid biosynthesis. A colorful model for genetics, biochemistry, cell biology, and biotechnology. Plant Physiol. **126:** 485–493.

Xie, D.-Y., Sharma, S.B., Paiva, N.L., Ferreira, D., and Dixon, R.A. (2003). Role of anthocyanidin reductase, encoded by BANYULS in plant flavonoid biosynthesis. Science **299:** 396–399.

Yang, P., Fu, H., Walker, J., Papa, C.M., Smalle, J., Ju, Y.M., and Vierstra, R.D. (2004). Purification of the *Arabidopsis* 26 S proteasome: Biochemical and molecular analyses revealed the presence of multiple isoforms. J. Biol. Chem. **279:** 6401–6413.

Yasuhara, M., Mitsui, S., Hirano, H., Takanabe, R., Tokioka, Y., Ihara, N., Komatsu, A., Seki, M., Shinozaki, K., and Kiyosue, T. (2004). Identification of ASK and clock-associated proteins as molecular partners of LKP2 (LOV kelch protein 2) in *Arabidopsis*. J. Exp. Bot. **55:** 2015–2027.

Zhang, K.W., Bhuiya, M.W., Pazo, J.R., Miao, Y., Kim, H., Ralph, J., and Liu, C.-J. (2012). An engineered monolignol 4-*O*-methyltransferase depresses lignin biosynthesis and confers novel metabolic capability in *Arabidopsis*. Plant Cell **24:** 3135–3152.

Zhao, D., Han, T., Risseeuw, E., Crosby, W.L., and Ma, H. (2003). Conservation and divergence of ASK1 and ASK2 gene functions during male meiosis in *Arabidopsis thaliana*. Plant Mol. Biol. **53:** 163–173.

Zhao, Q., and Dixon, R.A. (2011). Transcriptional networks for lignin biosynthesis: More complex than we thought? Trends Plant Sci. **16:** 227–233.

Zhong, R., and Ye, Z.H. (2007). Regulation of cell wall biosynthesis. Curr. Opin. Plant Biol. **10:** 564–572.